DETECTING SYMMETRY-BREAKING BIFURCATION POINTS OF SYMMETRIC STRUCTURES

C. CARSTENSEN* AND W. WAGNER[†]

*Institut für Angewandte Mathematik and [†]Institut für Baumechanik und Numerische Mechanik, Universität Hannover, Appelstr. 9A D-3000 Hannover 1, F.R.G.

SUMMARY

In engineering applications often problems with symmetric system and symmetric loading occur. It is well known that these symmetry conditions can be used to reduce the computational effort. Thus, only a symmetric reduced system is treated with sufficient boundary and loading conditions. Especially for non-linear problems this procedure is very effective. Such a strategy allows the computation of solution paths with the constraint that the solution has to be symmetric. Consequently in a stability analysis, only limit points and bifurcation points with associated symmetrical eigenvectors can be found. Often the stability behaviour is dominated by symmetry-breaking bifurcation points which cannot be detected considering only the tangent stiffness matrix of the reduced system. Hence, in case of stability considerations a calculation of the complete system is necessary. This paper introduces a special form of stability analysis of the complete system using only certain matrices known from the symmetric reduced system, and some transformations concerning the topology of the total system. The proposed methods base on a substructure technique for symmetry under reflections and rotations, and are formulated for the finite element method. Numerical examples are given to show the efficiency of the proposed procedures and algorithms.

1. INTRODUCTION

In engineering applications, often symmetric systems with symmetric loading and symmetric boundary conditions appear. Within an efficient computation of such problems—e.g. with the finite element method— -this symmetry can be used to reduce the computational costs. Especially for non-linear problems, where the solutions are achieved by incremental/iterative procedures, this aspect can be very important. Such iterative solution procedures base, in general, on path-following procedures together with Newton–Raphson's algorithm. Within these strategies the main computational effort in the solution process of the incremental linearized equations is dominated by the $\mathbf{LDL}^T$-reduction of the tangent stiffness matrix $\mathbf{K}_T$ which has to be calculated in all load steps and in each iteration step (for full Newton schemes).

Besides the calculation of the non-linear response of the system using, e.g., path following methods, one has to discuss the stability behaviour of the total structure. Typical stability effects are the appearence of limit or bifurcation points which can be detected by the singularity of the tangent stiffness matrix $\mathbf{K}_T$. The condition $\det \mathbf{K}_T = 0$ can easily be checked in each iteration step considering all signs of the pivot entries D_{ii} in the $\mathbf{LDL}^T$-reduction of $\mathbf{K}_T$. If the main interest is on the primary path, which can be proved mathematically to be symmetric,[1,2] it is sufficient to use only a symmetric reduced system.

Using such a symmetric reduced system only limit points or bifurcation points with symmetric zero eigenvectors can be detected. Within this discussion the type of bifurcation point can be symmetric or asymmetric[3] (truss and cylindrical shell example).

On the other hand, bifurcation points with unsymmetric eigenvectors cannot be found using the symmetric reduced system. Consequently, a discussion of the stability behaviour of the total system requires the control of its tangent stiffness matrix $\mathbf{K}_T$.

This paper considers the efficient calculation of the symmetric primary branch using the symmetric reduced system but enlarges the approach such that any singularity of the total system, e.g. a symmetry-breaking bifurcation point, is detected. The advantage of the proposed strategy will be explained considering the general algorithm as shown in Box 1.

Box 1. Algorithm 1

For any load level:

(1) Newton–Raphson's method:
    (1a) Compute residual $\mathbf{G}$.
    (1b) Compute $\mathbf{K}_T$ and its $\mathbf{LDL}^T$-decomposition.
    (1c) Solve linear equation $\mathbf{K}_T \Delta \mathbf{v} = -\mathbf{G}$.
    (1d) Update displacements $\mathbf{v}$.

(2) Stability considerations, for example discuss sign of all D_{ii}.

The main computational costs during a Newton–Raphson step are caused by the $\mathbf{LDL}^T$-decomposition which are denoted by c for the tangent stiffness matrix $\mathbf{K}_T^{RS}$ of the symmetric reduced system (RS) and κc for the tangent stiffness matrix $\mathbf{K}_T^{CS}$ of the complete structure (CS), respectively.

The difference between both calculations can be discussed in the following example. Let the dimension of $\mathbf{K}_T^{CS}$ be twice of $\mathbf{K}_T^{RS}$. Then, κ depends on the structure of $\mathbf{K}_T^{CS}$ and $\mathbf{K}_T^{RS}$ and may be bounded by

$$2 \leqslant \kappa \leqslant 8 \tag{1}$$

To see this, assume first that $\mathbf{K}_T^{CS}$ and $\mathbf{K}_T^{RS}$ have non-vanishing entries such that $c = O(n^3)$ and $\kappa c = O((2 \cdot n)^3) = 8 O(n^3) \approx 8c$, $n := \dim \mathbf{K}_T^{RS}$; here $O(\ )$ denotes the Landau symbols which cannot be confused with the n-dimensional orthogonal group $O(n)$. This gives an upper bound for κ. To determine the lower bound, assume that $\mathbf{K}_T^{CS}$ and $\mathbf{K}_T^{RS}$ are band-matrices with the same bandwidth, say, k. Then $c = O(k^2 n)$ and $\kappa c = O(k^2 2n) \approx 2c$. This proves equation (1).

As mentioned above, the computation of the total structure needs no additional stability considerations—the sign of the D_{ii}^{CS} can be seen automatically during the elimination process. Therefore, the computational costs of Algorithm 1 at a certain load level are nearly

$$5 \cdot \kappa \cdot c \tag{2}$$

Here, we have assumed that 5 iteration steps have to be done, for any load level which is typical for a full Newton scheme.

The computations using the symmetric reduced system gives no information on the symmetry-breaking bifurcation behaviour. Thus, at each load level an additional calculation and decomposition of $\mathbf{K}_T^{CS}$ with costs κc is necessary for the stability analysis. In total we have in our model situation costs of κc and $5 \cdot c$ for five Newton–Raphson steps. Thus, the computational costs of Algorithm 1 using the symmetric reduced system for one load level are nearly less than

$$5 \cdot c + \kappa c \tag{3}$$

Consequently, using the symmetric reduced system the computational effort is reduced in relation

to the computations with the total structure by a factor

$$\eta := \frac{5c + \kappa c}{5\kappa c} = \frac{1}{\kappa} + 0.2 \quad \text{with} \quad 0.325 \leqslant \eta \leqslant 0.7 \tag{4}$$

We have omitted in this process the calculation of $\mathbf{K}_T$ and $\mathbf{G}$ in comparison to the decomposition procedure.

Based on this preliminary considerations we introduce, in this paper, an algorithm for the required stability discussion of the total system in Algorithm 1 which is based on the particular structure of $\mathbf{K}_T$ in the presence of symmetry.

The paper is organized as follows. In Section 2 some basic equations for the description of the FEM are introduced. Then, Section 3 treats reflections where we derive that the stability test concerns only the singularity of two tangent stiffness matrices: one is the tangent stiffness matrix $\mathbf{K}_T^{RS}$ of the symmetric reduced system, while the second matrix is build by the antisymmetric boundary conditions. Furthermore, the case of a double-reflection symmetry is discussed in Section 4 where the regularity of four tangent stiffness matrices related to the symmetric reduced system must be checked for the stability of the total structure.

The rest of the paper concerns the symmetry by rotation which is more complicated and requires some preliminaries. In Section 5 we consider symmetric substructures and derive the equations for the symmetric reduced system in the case of symmetry by rotation. Especially, we determine boundary conditions defining the symmetric substructure. This enables the Newton–Raphson algorithm for the symmetric reduced system. We present Algorithm 3 for the detection of singular points of the total system only using the tangent stiffness matrix of one symmetric reduced system and the informations of the coupling behaviour between all substructures. Some informations about the relation of the zero eigenvectors of the total structure and the symmetric reduced system are also given. In Sections 4 and 5 some numerical examples are given illustrating the large reduction of the computational costs in comparison with a computation based on the total structure. Finally, some conclusions are drawn in Section 6.

2. BASIC EQUATIONS

This section describes the basic equations for the finite element formulation used in the subsequent sections.

The weak form of equilibrium of an elastic body under given loading can be written by the principle of virtual work with respect to the reference configuration B

$$\int_{(B)} (\delta \mathbf{E} \cdot \mathbf{S} - \delta \mathbf{u} \cdot \bar{\mathbf{b}}) \, dV - \int_{(\partial B_\sigma)} \delta \mathbf{u} \cdot \bar{\mathbf{t}} \, dA = 0 \tag{5}$$

with the displacement field $\mathbf{u}$, the Green–Lagrangian strains $\mathbf{E}$, the second Piola–Kirchhoff stresses $\mathbf{S}$ and the given body forces $\bar{\mathbf{b}}$ and surface tractions $\bar{\mathbf{t}}$. $\delta \mathbf{u}$ and $\delta \mathbf{E}$ are the virtual displacements and strains. The surface tractions $\bar{\mathbf{t}}$ acts on a part ∂B_σ of the boundary $\partial B = \partial B_\sigma \cup \partial B_u$ of the body B while the virtual displacements $\delta \mathbf{u}$ vanish at the other part ∂B_u.

The finite element discretization consists in restricting the displacements to a finite-dimensional, say n, space. On element level, the displacement field $\mathbf{u}_e$ is defined by

$$\mathbf{u}_e = \mathbf{N}_e \mathbf{v}_e \tag{6}$$

with a matrix $\mathbf{N}_e$ of shape functions and a nodal displacement vector $\mathbf{v}_e$. The associated virtual Green–Lagrangian strains are

$$\delta \mathbf{E}_e = \mathbf{B}_e \delta \mathbf{v}_e \quad \text{with} \quad (\mathbf{B} = \mathbf{B}_L + \mathbf{B}_{NL})_e \tag{7}$$

whereas the second Piola–Kirchhoff stresses are defined for a linear elastic material behaviour by

$$S_e = DE_e = D(B_L + 1/2B_{NL})_e v_e \tag{8}$$

Taking the discrete quantities in the principle of virtual work and summation on all elements leads to

$$\delta v^T G = \bigcup_{e=1}^{n_e} \delta v_e^T \left\{ \int_{(\Omega_e)} B_e^T S_e \, d\Omega - \int_{(\Omega_e)} N_e^T \bar{b} \, d\Omega - \int_{(\partial\Omega_e)} N_e^T d\bar{t}(\partial\Omega) \right\} = 0 \tag{9}$$

If we introduce an additional load parameter λ we end up with the well-known non-linear set of equations for the residual

$$G(v, \lambda) = R(v) - \lambda P = 0, \quad v \in \mathbb{R}^n, \lambda \in \mathbb{R} \tag{10}$$

with

$$R(v) = \bigcup_{e=1}^{n_e} \int_{(\Omega_e)} B_e^T S_e \, d\Omega, \quad P = \bigcup_{e=1}^{n_e} \left\{ \int_{(\Omega_e)} N_e^T \bar{b} \, d\Omega + \int_{(\partial\Omega_e)} N_e^{TT} \bar{t} \, d\partial\Omega \right\} \tag{11}$$

Throughout this paper, we assume that the solution of $G = R(v) - \lambda P = 0$ is computed by incremental path following methods. This requires a further constraint $f(v, \lambda) = 0$ to obtain a system of equations with locally unique solutions. Then the system can be solved by, e.g., Newton–Raphson's method where we compute the tangent stiffness matrix K_T, i.e. the Jacobian matrix of R. We refer e.g. to References 3–8 for a more detailed description of arc-length methods.

Using the implicit function theorem one concludes that the solution set of the equation $G = R(v) - \lambda P = 0$ is locally a path, if the tangent stiffness matrix K_T is regular. Consequently, any stability point $(\bar{v}, \bar{\lambda})$ fulfils $\det K_T = 0$.

Moreover, the stability of an equilibrium point (v, λ), i.e. $G(v, \lambda) = 0$, is said to be stable, singular or unstable, iff K_T is positive-definite, singular, or of some other form, respectively. This criterion can be applied if, e.g., a LDL^T-decomposition of the tangent stiffness matrix is known. If, correspondingly, all D_{ii} are positive, one D_{ii} vanishes, one D_{ii} is negative, then the equilibrium point (v, λ) is stable, singular, unstable. Thus, in view of Algorithm 1 the stability considerations can be done without additional effort if the complete system is treated. On the other hand, using a symmetric reduced system for the computation of symmetric solutions the tangential stiffness matrix of the full system is not known and further considerations are required.

3. REFLECTION SYMMETRY

In this section we discuss a finite-dimensional system of non-linear equations

$$G(v, \lambda) = 0 \tag{12}$$

where $G: \mathbb{R}^n \times \mathbb{R} \to \mathbb{R}^n$ is smooth. In addition we assume the presence of a reflection symmetry which is described by a linear orthogonal mapping $S \in O(n)$, $O(n)$ is the orthogonal group in $\mathbb{R}^n$, such that $S \neq I$ but $SS = I$, I is the unity in $\mathbb{R}^n$ and identified with the n-dimensional unit matrix.

The key is a decomposition of the displacement vector in $\mathbb{R}^n$ in symmetric, denoted by V_s, and antisymmetric displacements, denoted by V_a, i.e.

$$V_s := \{ v \in \mathbb{R}^n \mid Sv = v \}, \quad V_a := \{ v \in \mathbb{R}^n \mid Sv = -v \} \tag{13}$$

Any displacement field can be defined as a sum of a symmetric and an antisymmetric displacement field which can be written for the related vectors as

$$V_s \bigoplus V_a = \mathbb{R}^n \tag{14}$$

Example. Assume that **G** represents equilibrium of a (discrete) mechanical structure Ω in global co-ordinates which is symmetric under reflection with respect to the y-axis, say, such that

$$\mathbf{S}' = \begin{pmatrix} 1 & & \\ & -1 & \\ & & 1 \end{pmatrix} \tag{15}$$

Then, the symmetry of Ω can be written as follows. There exists a substructure Ω_1 which is mapped by $\mathbf{S}'$ onto $\Omega_2 = \mathbf{S}'\Omega_1$ such that $\Omega = \Omega_1 \cup \Omega_2$. Moreover, the symmetry yields the displacements $\mathbf{v}: \Omega \to \mathbb{R}^3$ being symmetric, i.e. $\mathbf{v} \in V_s$, if and only if the restriction of $\mathbf{v}$ to Ω_1, denoted by $\mathbf{v}_1 := \mathbf{v}|_{\Omega_1}$, represents $\mathbf{v}$ according to

$$\mathbf{v}(x) = \mathbf{v}_1(x) \quad \text{if } x \in \Omega_1 \quad \text{and} \quad \mathbf{v}(x) = \mathbf{S}\mathbf{v}_1(x) \quad \text{if } x \in \Omega_2 \tag{16}$$

Therefore, as it is well-known for engineers we can restrict the computation of symmetric displacements to the half Ω_1 of the system, if we add suitable symmetric boundary conditions to Ω_1. These symmetric boundary conditions can be computed by the condition $\mathbf{v}(x) = \mathbf{v}_1(x) = \mathbf{v}_2(x)$ for all $x \in \Omega_1 \cap \Omega_2$. This yields $\mathbf{S}'\mathbf{u}(x) = \mathbf{u}(x)$ for the allowed displacements $\mathbf{u}(x) \in \mathbb{R}^3$ at a point $x \in \Omega_1 \cap \Omega_2$ of the symmetric boundary. In the present example $\mathbf{S}'\mathbf{u}(x) = \mathbf{u}(x)$ means that $u_1(x), u_3(x)$ are arbitrary while $u_2(x) = 0$. This confirms the engineering approach.

Remarks. (i) The symmetry $\mathbf{S}'$ of the above example depends on the degrees of freedom which are three in the example (e.g. a 3-D solid problem). If we add three rotations to describe 3-D beam problems for instance than $\mathbf{S}'$ becomes a diagonal matrix of dimension six with the diagonal entries $1, -1, 1, -1, 1, -1$.

(ii) We refer the mechanical system Ω_1 with the symmetric boundary conditions to the *symmetric reduced system*. Analogously, the mechanical system Ω_1 with the antisymmetric boundary conditions (these are the symmetric conditions of $-\mathbf{S}'$) is called the *antisymmetric reduced system*.

(iii) We emphasize that the symmetry $\mathbf{S}'$, like equation (15), describes the system in some sense in local co-ordinates $\mathbf{u}$ while $\mathbf{S}$ represents the symmetry for the displacement vectors $\mathbf{v}$ and, hence in some sense in global co-ordinates. Obviously $\mathbf{S}' \neq \mathbf{S}$ (the dimensions do not coincide). On the other hand, both $\mathbf{S}$ and $\mathbf{S}'$ represent the same symmetry. Therefore, in mathematical literature,[1, 2, 8, 9] $\mathbf{S}$ is called the *action* of $\mathbf{S}'$. For our engineering approach this is not important, because for the case of symmetry under reflection the situation is clear.

The fact that the system is symmetric often gives the following symmetry condition for all $\mathbf{v} \in \mathbb{R}^n$ and all $\lambda \in \mathbb{R}$

$$\mathbf{G}(\mathbf{S}\mathbf{v}, \lambda) = \mathbf{S}\mathbf{G}(\mathbf{v}, \lambda) \tag{17}$$

To give an example we consider an energy approach.[2] Let $\mathbf{G}(\mathbf{v}, \lambda)$ be of the form of the previous section, namely,

$$\mathbf{G}(\mathbf{v}, \lambda) = \mathbf{R}(\mathbf{v}) - \lambda\mathbf{P} \quad \text{with} \quad \mathbf{R}(\mathbf{v}) = D_v \Pi_i(\mathbf{v}) \tag{18}$$

In this situation the symmetry condition (17) is satisfied if the load is symmetric, i.e.

$$\mathbf{S}\mathbf{P} = \mathbf{P} \tag{19}$$

and the internal energy is symmetric, i.e.

$$\Pi_i(\mathbf{S}\mathbf{v}) = \Pi_i(\mathbf{v}) \quad \text{for all } \mathbf{v} \in \mathbb{R}^n \tag{20}$$

Lemma 1. *For* **G** *from equation (18) a symmetric energy (20) and loading (19) imply the symmetry condition (17).*

Proof. Differentiation of equation (20) gives

$$\mathbf{R}(\mathbf{v}) = D_v \Pi_i(\mathbf{v}) = D_v \Pi_i(\mathbf{S}\mathbf{v}) = \mathbf{S}^T \mathbf{R}(\mathbf{S}\mathbf{v}) \tag{21}$$

by the chain rule. Multiplication with **S** proves equation (17). ∎

The symmetry condition (17) is usually required in the mathematical literature to which we refer for a mathematical treatment of the rest of this section.[7-9]

Using equation (17) the following lemma[7] is known, the proof is given for completeness.

Let $\mathbf{K}_T$ be the tangent stiffness matrix, i.e. $\mathbf{K}_T := D_v \mathbf{G}(\mathbf{v}, \lambda)$.

Lemma 2. *On the symmetric primary path,* $\mathbf{K}_T$ *always has a symmetric or an antisymmetric zero eigenvector whenever it is singular.*

Proof. Since $\mathbf{K}_T$ is singular there exists a zero eigenvector $\varphi \neq 0$. In case $\varphi \in V_s$, the lemma is already proved. Otherwise $\phi := \varphi - \mathbf{S}\varphi$ is non-zero. Note that $\phi \in V_a$ since

$$\mathbf{S}\phi = \mathbf{S}\varphi - \mathbf{S}\mathbf{S}\varphi = \mathbf{S}\varphi - \varphi = -\phi \tag{22}$$

It remains to prove that ϕ is also a zero eigenvector. Differentiation of equation (17) gives

$$D_v \mathbf{G}(\mathbf{S}\mathbf{v}, \lambda)\mathbf{S} = \mathbf{S}D_v\mathbf{G}(\mathbf{v}, \lambda) \tag{23}$$

Since we are on the symmetric primary path there holds $\mathbf{v} = \mathbf{S}\mathbf{v}$, and hence $\mathbf{K}_T$ denotes $D_v\mathbf{G}(\mathbf{v}, \lambda)$,

$$\mathbf{K}_T \mathbf{S} = \mathbf{S}\mathbf{K}_T \tag{24}$$

which implies

$$\mathbf{K}_T \mathbf{S}\varphi = \mathbf{S}\mathbf{K}_T\varphi = 0 \tag{25}$$

Thus, $\mathbf{S}\varphi$ is a zero eigenvector as well as ϕ. ∎

Lemma 2 states that any singularity of the total structure gives a symmetric or antisymmetric zero eigenvector of the total system. Any symmetric or antisymmetric zero eigenvector of $\mathbf{K}_T$ gives an eigenvector of the tangent stiffness matrix of the symmetric reduced system at the symmetric primary path including the symmetric or antisymmetric boundary conditions.

Altogether, any singular point of the total system can be detected by the following algorithm which defines the part 'stability considerations' in Algorithm 1.

Box 2. Algorithm 2

(a) Compute the tangent stiffness matrix of the reduced system without any boundary condition.

(b) Add all global boundary conditions of the structure which are also relevant for the symmetric structure. Denote the resulting tangent stiffness matrix by **K**.

(c) Take **K** and add the symmetric boundary conditions along the symmetry plane giving the tangent matrix $\mathbf{K}_T^s$ of the symmetric reduced system (which is computed in any step of Newton–Raphson's algorithm). Compute a decomposition of $\mathbf{K}_T^s$.

(d) Take **K** and add the antisymmetric boundary conditions along the symmetry plane giving the tangent matrix $\mathbf{K}_T^a$ of the antisymmetric reduced system. Compute a decomposition of $\mathbf{K}_T^a$.

(e) Output: If all pivots in (c) and (d) are positive, then $\mathbf{K}_T$ is positive-definite; the total system is stable. If some pivot elements in (c) or (d) becomes zero or negative, $\mathbf{K}_T$ is singular or the total system is unstable.

Remark. Algorithm 2 solves the problem for symmetry by reflection and can easily be implemented in existing computer programs. Note that the positive-definiteness of $\mathbf{K}_T^s$ is checked during the Newton–Raphson steps so that only one additional test has to be introduced with the same computational effort as one Newton–Raphson iteration. Consequently, as in the example discussed in Section 1, using Algorithms 1 and 2 for the symmetric reduced system, the computational costs are reduced in relation to the total structure by a factor

$$\eta' := \frac{5c + c}{5\kappa c} = \frac{6}{5 \cdot \kappa} \quad \text{with} \quad 0.15 \leqslant \eta' \leqslant 0.6 \tag{26}$$

Remark. The computational costs using Algorithms 1 and 2 can further be reduced by the following procedure. Change the coefficients in $\mathbf{K}_T$ of dimension n such that the nodes of the symmetry axis correspond to the last r components, $n = l + r$. Then, computing a $\mathbf{LDL}^T$-decomposition of $\mathbf{K}_T$ for the Newton–Raphson iteration break after the elimination of the first l columns and store the submatrix, denoted by $\mathbf{K}_T' \in \mathbb{R}^{r \times r}$, in the positions of the last r rows and columns. Then, take the boundary condition in (c) or (d) in Algorithm 2, delete the corresponding rows and columns in $\mathbf{K}_T'$ to obtain $\mathbf{K}_T''$ and compute a $\mathbf{LDL}^T$-decomposition of $\mathbf{K}_T''$. Consider the diagonal entries in this decomposition. If they are all positive [in all cases of (c) and (d)], then the total system is stable.

4. DOUBLE REFLECTION SYMMETRY

We continue the consideration of the previous section assuming that, in addition, there exist two reflection symmetries which are described by two linear orthogonal mappings $\mathbf{S}_1, \mathbf{S}_2 \in O(n)$, $\mathbf{S}_i \neq \mathbf{I}$ but $\mathbf{S}_i \mathbf{S}_i = \mathbf{I}$ and $\mathbf{S}_i$ satisfies the symmetry condition (17) ($i = 1, 2$).

Example. We refer to Reference 3 for a stability analysis of cylindrical shell segment under axial loading. Due to the double reflection symmetry, only one quarter of the segment has been discretized.

As in the previous section, we decompose the displacements $\mathbb{R}^n$ in symmetric and antisymmetric displacements with respect to $\mathbf{S}_1$ and $\mathbf{S}_2$ as follows:

$$V_{ss} := \{\mathbf{v} \in \mathbb{R}^n | \mathbf{S}_1 \mathbf{v} = \mathbf{v} \quad \text{and} \quad \mathbf{S}_2 \mathbf{v} = \mathbf{v}\} \tag{27}$$

$$V_{sa} := \{\mathbf{v} \in \mathbb{R}^n | \mathbf{S}_1 \mathbf{v} = \mathbf{v} \quad \text{and} \quad \mathbf{S}_2 \mathbf{v} = -\mathbf{v}\} \tag{28}$$

$$V_{as} := \{\mathbf{v} \in \mathbb{R}^n | \mathbf{S}_1 \mathbf{v} = -\mathbf{v} \quad \text{and} \quad \mathbf{S}_2 \mathbf{v} = \mathbf{v}\} \tag{29}$$

$$V_{aa} := \{\mathbf{v} \in \mathbb{R}^n | \mathbf{S}_1 \mathbf{v} = -\mathbf{v} \quad \text{and} \quad \mathbf{S}_2 \mathbf{v} = -\mathbf{v}\} \tag{30}$$

Again, it can be seen that

$$V_{ss} \bigoplus V_{sa} \bigoplus V_{as} \bigoplus V_{aa} = \mathbb{R}^n. \tag{31}$$

We apply Lemma 2 to $\mathbf{S}_i$, for $i = 1$ and $i = 2$ and obtain the following lemma.

Lemma 3. On the symmetric primary path, $\mathbf{K}_T$ always has a non-zero eigenvector in one of the four spaces V_{ss}, V_{sa}, V_{as}, V_{aa} whenever $\mathbf{K}_T$ is singular.

By Lemma 3, any singular point of the total system can be detected by the algorithm which defines the part 'Stability considerations' by Algorithm 2 except that in step (c) and (d) we have to consider four boundary conditions which are given by (c) and (d) in Algorithm 2 applied with respect to $\mathbf{S}_1$ and $\mathbf{S}_2$, respectively.

At the end of this section we discuss a shell problem with reflection symmetries in detail. Finally, we discuss the computational effort.

Remarks. The computational effort for the proposed procedure can be improved as mentioned in the last remark where we have to check four cases. One of them is done during the Newton–Raphson iteration. Then, the computational costs are reduced in relation to the computations with the total structure by a factor

$$\eta' := \frac{5c + 3c}{5\kappa c} = 1\cdot 6/\kappa \tag{32}$$

Here, the dimension of the total system is four times greater than the reduced system yielding $4 \leqslant \kappa \leqslant 64$ and

$$0\cdot 025 \leqslant \eta'' \leqslant 0\cdot 4 \tag{33}$$

Example. As an example to the above-formulated reflection symmetry, we consider the calculation of a symmetry breaking bifurcation point of a non-linear shell problem. For this purpose, we discuss the non-linear structural behaviour of cylindrical shell segment under a uniform transverse load. All edges of the segment are clamped. The geometrical and material data are given in Figure 1.

All in this paper discussed algorithms and finite element formulations are introduced in the finite element program **FEAP** described in Zienkiewicz and Taylor.[10] The employed element is presented in References 11, 12. All known results base on the introduction of a double symmetry.[13, 14] Thus, only one-quarter of the system is used within the finite element analysis. The associated load–deflection curve for the centre deflection w_c is stated in Figure 2 for a 4×4 (reduced) mesh.

Own calculations[15] show that using the complete system a symmetry breaking bifurcation point occur at a load level of $p = 1\cdot 802$ kN/m². (remark: this result can be achieved with one-half of the system too!) In Figure 3 the relevant part of the load–deflection path is shown. Between the symmetry breaking bifurcation point ($p = 1\cdot 802$ kN/cm², $w_c = 5\cdot 490$ mm) and the bifurcation point ($p = 3\cdot 052$ kN/cm², $w_c = 11\cdot 033$ mm) we have an symmetric and an antisymmetric solution branch, which can be seen in Figure 3 in detail.

The associated deformation behaviour is characterized by the first two eigenvectors—calculated in the symmetry-breaking bifurcation point (see Figure 4). The null eigenvector φ_1 defines the antisymmetric deformation behaviour whereas the second eigenvector φ_2 belongs to the symmetric path.

The different behaviour on both paths can be seen clearly if we look at the load–deflection paths for the points L and R (see Figure 4). Thus, we have in Figure 5 one symmetric solution ($w_L = w_R$) and two antisymmetric solutions ($w_L \neq w_R$).

$E = 3102.75\,N/mm^2$
$\nu = 0.3$
$\Theta = 0.1\,rad$
$t = 3.175\,mm$
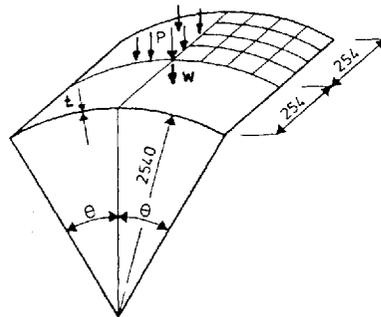$\Delta p = 1\,kN/m^2$

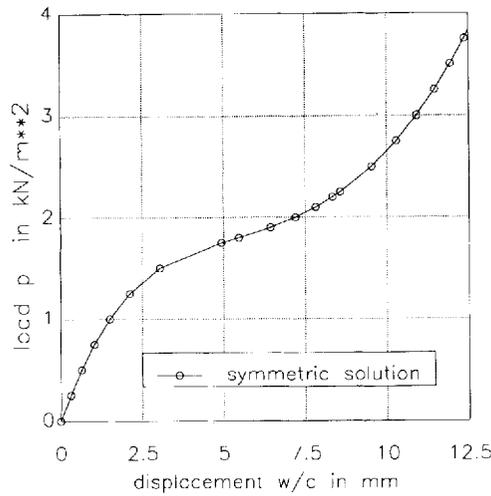Figure 1. Cylindrical shell segment under uniform load

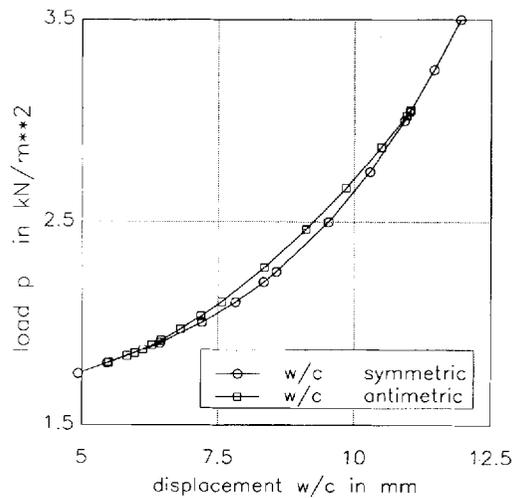Figure 2. Symmetrical load–deflection path p-w_c

Figure 3. Symmetric and antisymmetric load–deflection paths p_1 w_c

To discuss the efficiency of the proposed algorithms we need computation times. For this purpose we run the program **FEAP** on a 386 PC (33 MHz). In Figure 6 we show the computation time for calculation and decomposition of the tangent stiffness matrix K_T depending on the number of elements for one side of the complete segment. Thus, for example, a reduced system with a 4×4 mesh belongs to a complete system with an 8×8 mesh.

From Figure 6 we check our estimates of the computational costs in equation (33). Indeed, κ can be computed using the numerical data in Figure 6 as the quotient of the times for the complete and reduced system. We have $\kappa = 6, 6\cdot33, 7\cdot94$ which can be compared with our bounds $4 \leqslant \kappa \leqslant 64$ and shows experimentally that the considered matrices of this example behaves more than band-matrices. From equation (32) we see that the computational costs are reduced in relation to the computations with the total structure by a factor $\eta'' := 0\cdot266, 0\cdot253, 0\cdot202$.
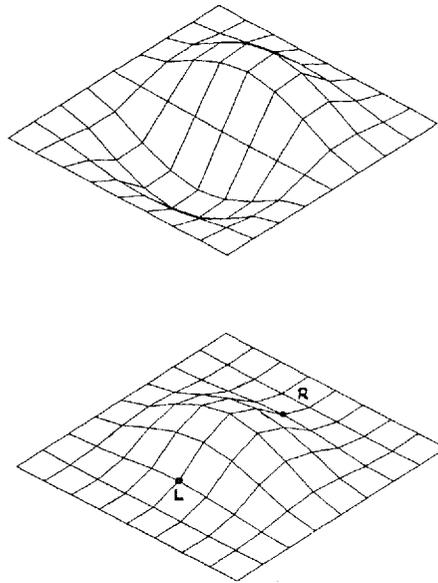
Figure 4. First and Second eigenvector φ_1 and φ_2 at the symmetry breaking bifurcation point
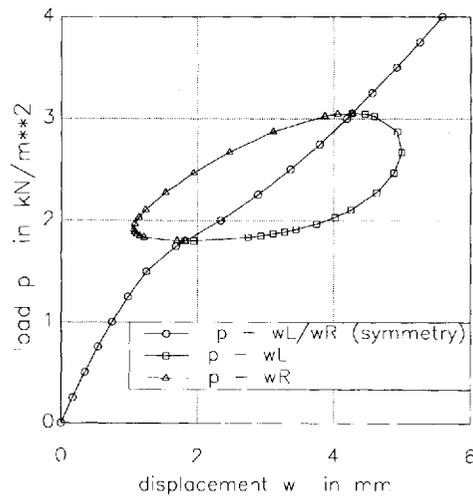

Figure 5. Symmetric and antisymmetric load–deflection paths p–w_s, p–w_L, p–w_R

5. SYMMETRIC SUBSTRUCTURES

This section gives a description of a structure and its substructures, specifies this to symmetric structures and defines the symmetric reduced system for rotation symmetry. Finally, we discuss in which way the singularity of the total system can be observed considering only the tangent stiffness matrix of the reduced system.
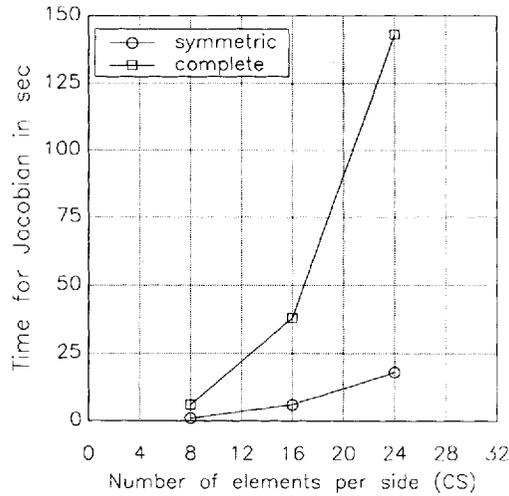
Figure 6. Time for computing $\mathbf{K}_T^{RS}$ and $\mathbf{K}_T^{CS}$ vs. elements per side

To describe substructures we come back to Section 2 and write the finite element discretization of the body B with ne elements $\Omega_1, \ldots, \Omega_{ne}$ as

$$B^h = \bigcup_{e=1}^{ne} \Omega_e \tag{34}$$

The substructures of B^h are given by the assembling process of some of the elements in groups or macroelements as follows. Write $\Omega_1^1, \ldots, \Omega_{ne^1}^1, \Omega_1^2, \ldots, \Omega_{ne^2}^2, \ldots, \Omega_1^m, \ldots, \Omega_{ne^m}^m$ for the elements $\Omega_1, \ldots, \Omega_{ne}$, $ne^1 + \cdots + ne^m = ne$, and define

$$\Omega^j := \bigcup_{e=1}^{ne^j} \Omega_e^j \quad (j = 1, \ldots, m) \tag{35}$$

such that

$$B^h = \bigcup_{j=1}^{m} \Omega^j = \bigcup_{j=1}^{m} \bigcup_{e=1}^{ne^j} \Omega_e^j \tag{36}$$

Since the order of the assembling process, written by the operator $\bigcup$, can be changed arbitrary the consideration of substructures $\Omega^1, \ldots, \Omega^m$ gives the same discretization B^h. The substructures can be handled as finite elements itself so that transformations, assembling procedures and connections of global and local co-ordinates can be written and implemented as for usual finite elements.

If $\mathbf{v}$ denotes the global displacement vector, we can arrange its components in the form

$$\mathbf{v} = (\mathbf{v}_1, \ldots, \mathbf{v}_m, \mathbf{w})^T \in \mathbb{R}^n \tag{37}$$

where $\mathbf{w}$ describes the components of such degrees of freedom that acts on two or more substructures while $\mathbf{v}_j$ describes the components of such degrees of freedom that acts on only one substructure Ω_j. Therefore, the principle of virtual work, introduced in Section 2, can be written as

$$\sum_{j=1}^{m} (\delta\mathbf{v}_j, \delta\mathbf{w}_j)^T \{ \mathbf{R}_j(\mathbf{v}_j, \mathbf{w}_j) - \lambda\mathbf{P}_j \} = 0 \tag{38}$$

Since v_j acts only in Ω^j we may assume that $\mathbf{v}^j$ is given in the local co-ordinate system of Ω^j. This, in general, is false for $\mathbf{w}_j$ which must be computed from $\mathbf{w}$ by a linear transformation $\mathbf{T}_j$, i.e.

$$\mathbf{w}_j = \mathbf{T}_j\mathbf{w} \quad \text{and} \quad \delta\mathbf{w}_j = \mathbf{T}_j\delta\mathbf{w} \tag{39}$$

In addition, we assume symmetric substructures under symmetric loads, i.e. the residuals $\mathbf{R}_j$ equals in local co-ordinates as well as the loading vectors $\mathbf{P}_j$,

$$\mathbf{R}_1 = \mathbf{R}_2 = \cdots = \mathbf{R}_m =:(\mathbf{R}_v, \mathbf{R}_w)^\mathsf{T} \quad \text{and} \quad \mathbf{P}_1 = \mathbf{P}_2 = \cdots = \mathbf{P}_m =:(\mathbf{P}_v, \mathbf{P}_w)^\mathsf{T}. \tag{40}$$

Here we split $\mathbf{R}_j$ and $\mathbf{P}_j$ in the components which are multiplied with $\delta\mathbf{v}_j$ and $\delta\mathbf{w}_j$ denoted by $\mathbf{R}_v$, $\mathbf{R}_w$ and $\mathbf{P}_v$, $\mathbf{P}_w$ respectively.

Then, the principle of virtual work for symmetric substructures on symmetric loading is

$$\sum_{j=1}^{m} \delta\mathbf{v}_j^\mathsf{T}[\mathbf{R}_v(\mathbf{v}_j, \mathbf{T}_j\mathbf{w}) - \lambda\mathbf{P}_v] + \delta\mathbf{w}^\mathsf{T}\mathbf{T}_j^\mathsf{T}[\mathbf{R}_w(\mathbf{v}_j, \mathbf{T}_j\mathbf{w}) - \lambda\mathbf{P}_w] = 0 \tag{41}$$

which yields (since $\delta\mathbf{v}_j$ and $\delta\mathbf{w}$ are arbitrary) the system of non-linear equations

$$\mathbf{R}_v(\mathbf{v}_j, \mathbf{T}_j\mathbf{w}) - \lambda\mathbf{P}_v = \mathbf{0} \quad (j = 1, \ldots, m) \tag{42}$$

and

$$\sum_{j=1}^{m} \mathbf{T}_j^\mathsf{T}\mathbf{R}_w(\mathbf{v}_j, \mathbf{T}_j\mathbf{w}) - \sum_{j=1}^{m} \lambda\mathbf{T}_j^\mathsf{T}\mathbf{P}_w = \mathbf{0} \tag{43}$$

As in the previous sections we are interested in the symmetric primary path. A vector $\mathbf{v}$ is called *symmetric* iff the local displacements $(\mathbf{v}_j, \mathbf{w}_j)$ equal, i.e. iff

$$\mathbf{v}_1 = \mathbf{v}_2 = \cdots = \mathbf{v}_n =:\mathbf{v}^* \quad \text{and} \quad \mathbf{w}_1 = \mathbf{w}_2 = \cdots = \mathbf{w}_m =:\mathbf{w}^* \tag{44}$$

Thus, $\mathbf{v}$ is symmetric iff there exist $\mathbf{v}^*$ and $\mathbf{w}^*$ with

$$\mathbf{v} = (\mathbf{v}^*, \ldots, \mathbf{v}^*, \mathbf{w})^\mathsf{T} \quad \text{and} \quad \mathbf{w}^* = \mathbf{T}_j\mathbf{w} \quad (j = 1, \ldots, m) \tag{45}$$

For symmetric displacements the following lemma is easily verified. Let

$$\mathbf{T}^* := \sum_{j=1}^{m} \mathbf{T}_j \tag{46}$$

Lemma 4. A symmetric vector $\mathbf{v}$ solves equations (42) and (43) iff

$$\mathbf{R}_v(\mathbf{v}^*, \mathbf{w}^*) - \lambda\mathbf{P}_v = \mathbf{0} \quad \text{and} \quad \mathbf{T}^{*\mathsf{T}}\mathbf{R}_w(\mathbf{v}^*, \mathbf{w}^*) - \lambda\mathbf{T}^{*\mathsf{T}}\mathbf{P}_w = \mathbf{0} \tag{47}$$

∎

Lemma 4 and the definition of symmetric displacements describe the *symmetric reduced system.* Obviously, to compute symmetric solutions of the primary path it requires to compute the related vector $(\mathbf{v}^*, \mathbf{w}^*)$ as a solution of equation (47). Since, e.g., $\mathbf{R}_1 = (\mathbf{R}_v, \mathbf{R}_w)^\mathsf{T}$, we can state the following mechanical interpretation of equation (47).

Definition. In the above notations of symmetric substructures under symmetric loading the *symmetric reduced system* is given as one substructure, e.g., Ω^1 with the boundary conditions for the local displacements $(\mathbf{v}_1, \mathbf{w}_1)$ given by

$$\mathbf{w}_1 \in \{\mathbf{w} | \exists\mathbf{W} \; \forall j = 1, \ldots, m \; \mathbf{w} = \mathbf{T}_j\mathbf{W}\} \tag{48}$$

and the load $\lambda(\mathbf{P}_v, \mathbf{T}^{*\mathsf{T}}\mathbf{P}_w)$.

The computation of the symmetric reduced system leads to all symmetric paths of the total system and reduces mostly the computational costs, since the dimension of the total system is approximately m times bigger than the dimension of the symmetric reduced system.

It remains to implement the reduced system, i.e. to compute the boundary conditions, which is illustrated in the following example.

Example. We consider the discrete structure of Figure 7 and let $\Omega^j \subset \mathbb{R}^3, j = 1, 2, 3$ correspond to the three equal beam members defined by the elements $(j - 1) \cdot 6 + 1, \ldots, j \cdot 6$.

The boundary conditions are given such that the three displacements of the nodes $1, 8, 14$ vanish. Based on the displacement field

$$\mathbf{u}(x) = (u_x, u_y, u_z, \varphi_x, \varphi_y, \varphi_z) \in \mathbb{R}^6 \tag{49}$$

the dimension of the global displacement vector $\mathbf{v}$ is $n = (19 \times 6) - (3 \times 3) = 105$. In the example we have

$$\mathbf{v} = (\mathbf{v}_1, \mathbf{v}_2, \mathbf{v}_3, \mathbf{w}) \quad \text{where} \quad \mathbf{v}_j \in \mathbb{R}^{33}, \mathbf{w} \in \mathbb{R}^6 \tag{50}$$

$\mathbf{v}_1, \mathbf{v}_2, \mathbf{v}_3$ and $\mathbf{w}$ represents the degrees of freedom of the node $1, \ldots, 6, 8, \ldots, 13, 14, \ldots, 19$ and 7, respectively. The local co-ordinate system of Ω_1 is shown in Figure 7 and given for Ω_j by rotations of $\pm 120°, j = 2, 3$. Therefore, we have, letting $c := \cos(120°), s := \sin(120°)$

$$\mathbf{T}_1 = \begin{pmatrix} 1 & & & & & \\ & 1 & & & & \\ & & 1 & & & \\ & & & 1 & & \\ & & & & 1 & \\ & & & & & 1 \end{pmatrix} \tag{51}$$

$$\mathbf{T}_2 = \begin{pmatrix} c & s & & & & \\ -s & c & & & & \\ & & 1 & & & \\ & & & c & s & \\ & & & -s & c & \\ & & & & & 1 \end{pmatrix} \tag{52}$$

$$EA = 10000$$

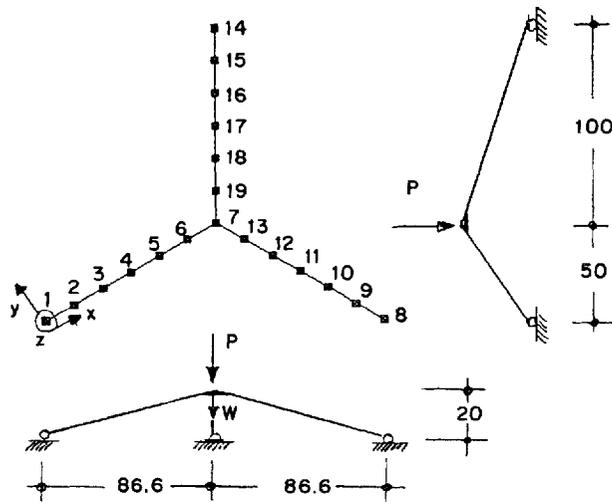$$EI_y = 20000$$

$$EI_z = 20000$$

$$GA_s = 500$$

$$GI_T = 100000$$

Figure 7. Three-dimensional beam problem with three members

$$T_3 = \begin{pmatrix} c & -s & & & & \\ s & c & & & & \\ & & 1 & & & \\ & & & c & -s & \\ & & & s & c & \\ & & & & & 1 \end{pmatrix} \qquad (53)$$

$$T_4 = \begin{pmatrix} 0 & & & & & \\ & 0 & & & & \\ & & 3 & & & \\ & & & 0 & & \\ & & & & 0 & \\ & & & & & 3 \end{pmatrix} \qquad (54)$$

Then the boundary conditions of the symmetric reduced system, given in equation (48), are equivalent to

$$\mathbf{w} = (0, 0, w_3, 0, 0, w_6)^{\mathbf{T}} \qquad (55)$$

where w_3 and w_6 are arbitrary real components. [For a proof note that if $\mathbf{w}$ satisfies equation (48) then $\mathbf{T}^*\mathbf{w} = 3\cdot\mathbf{w}$ implying the claimed form of $\mathbf{w}$ in equation (55). Conversely, if equation (55) holds it is easily verified that equation (48) holds.]

Note that the static boundary conditions are related with the loads $\mathbf{P}_v$ and $\mathbf{P}_w$. From Figure 7 we conclude that $\mathbf{P}_v = \mathbf{0}$ while we must define $\mathbf{P}_w = (0, 0, -P/3, 0, 0, 0)$ such that the sum of the loads of all substructures is $(0, 0, -P, 0, 0, 0)$.

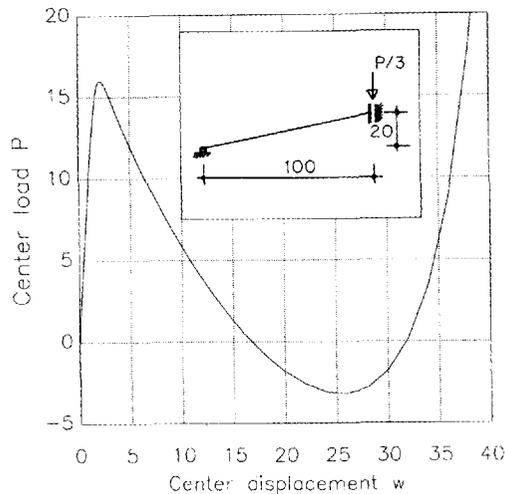This defines the symmetric reduced substructure which is shown in Figure 8.

Figure 8. Three-dimensional beam problem: λ w_3, primary branch

The static system can be analysed with a standard non-linear finite element program giving the λ-w_3 diagram of Figure 8 which concludes the example.

Note that the geometric boundary conditions in equation (55) corresponds to the static conditions, i.e. any degree of freedom in the node 7 which must be zero because of equation (55) gets no static condition while the static conditions concerns only the third or the last component of R_w.

According to the symmetric reduced system the symmetric primary path can be computed, but no further information about the stability of the total system is given. Therefore, some additional considerations and computations are needed which are described in the sequel. We first determine the tangent stiffness matrix K_T of the total system under the present notations of the symmetric substructures and then we reduce the question whether K_T is positive-definite or not using the above introduced terms of only one substructure and the transformation matrices.

Any solution vector v of the total system (symmetric or not) satisfies the equations (42) and (43). Differentiation of the residuals in equation (42) and (43) with respect to $v_1, \ldots, v_m, w$ gives the tangent stiffness matrix $K_T := D_v R(v^*, \ldots, v^*, w^*)$ of the total system

$$K_T = \begin{pmatrix} A & & & & BT_1 \\ & A & & & BT_2 \\ 0 & & \ldots & & \vdots \\ & & & A & BT_m \\ T_1^T C & T_2^T C & \ldots & T_m^T C & \sum_{j=1}^{m} T_j^T D T_j \end{pmatrix} \tag{56}$$

where we assumed that K_T is computed on the symmetric primary path, i.e. for a symmetric global displacement vector $(v^*, \ldots, v^*, w^*)$, and we used the abbreviations

$$A = D_v R_v(v^*, w^*) \tag{57}$$

$$B = D_w R_v(v^*, w^*) \tag{58}$$

$$C = D_v R_w(v^*, w^*) \tag{59}$$

$$D = D_w R_w(v^*, w^*) \tag{60}$$

Note that

$$K_T^S := \begin{pmatrix} A & B \\ C & D \end{pmatrix} \tag{61}$$

is the tangent stiffness matrix of the symmetric reduced system after the assembling process such that the global boundary conditions are treated but the conditions (48) are ignored. Consequently, most of the entries in K_T are known from the symmetric reduced system.

Let K_T^{RS} denote the tangential stiffness matrix of the symmetric reduced system. Note that K_T^{RS} is a submatrix of K_T^S.

The following lemma gives a sufficient condition for the Theorem 1 below which will solve the question whether K_T is positive-definite or not.

Lemma 5. If the symmetric reduced system is stable then D is positive-definite.

Proof. As mentioned above, K_T^{RS} is a submatrix of K_T^S and obtained by treating the boundary conditions (48). Since this boundary conditions do not concern the submatrix A (consisting of inner nodes) A is also a submatrix of K_T^{RS}. Then, by assumption, A is a (symmetric) submatrix of a positive-definite matrix K_T^{RS} and, therefore, itself positive-definite. ∎

Theorem 1. *If* $\mathbf{A}$ *is positive-definite, then the number of negative eigenvalues of* $\mathbf{K}_T$ *is equal to the number of negative eigenvalues of*

$$\mathbf{K}^* := \sum_{j=1}^{m} \mathbf{T}_j^T (\mathbf{D} - \mathbf{C}\mathbf{A}^{-1} \cdot \mathbf{B}) \mathbf{T}_j \tag{62}$$

Proof. Let the blocks in $\mathbf{K}_T$ corresponding to $(\mathbf{v}_1, \ldots, \mathbf{v}_m)$ and $\mathbf{w}$ be defined as follows

$$\mathbf{K}_T =: \begin{pmatrix} \hat{\mathbf{A}} & \hat{\mathbf{B}} \\ \hat{\mathbf{C}} & \hat{\mathbf{D}} \end{pmatrix} \tag{63}$$

$\hat{\mathbf{D}}$ is block diagonal with m diagonal blocks $\mathbf{A}$ and hence $\hat{\mathbf{A}}$ is positive-definite. Then, simple calculations prove

$$\begin{pmatrix} \mathbf{I} & \\ -\hat{\mathbf{C}}\hat{\mathbf{A}}^{-1} & \mathbf{I} \end{pmatrix} \begin{pmatrix} \hat{\mathbf{A}} & \hat{\mathbf{B}} \\ \hat{\mathbf{C}} & \hat{\mathbf{D}} \end{pmatrix} \begin{pmatrix} \mathbf{I} & -\hat{\mathbf{A}}^{-1}\hat{\mathbf{B}} \\ & \mathbf{I} \end{pmatrix} = \begin{pmatrix} \hat{\mathbf{A}} & \\ & \mathbf{K}^* \end{pmatrix} \tag{64}$$

where $\mathbf{I}$ denotes unit matrices of sufficient and, hence, different dimensions. Since $\mathbf{K}_T$ is symmetric, the last identity is a unitary transformation such that (due to a well-known theorem of Sylvester) the number of negative eigenvalues of $\mathbf{K}_T$ and that of the last matrix are equal. By assumption $\hat{\mathbf{A}}$ is positive-definite so that the number of negative eigenvalues of $\mathbf{K}_T$ is equal to the number of negative eigenvalues of $\mathbf{K}^*$.   ∎

Based on Theorem 1 we can formulate the following algorithm which computes $\mathbf{K}^*$ and a $\mathbf{LDL}^T$ decomposition of $\mathbf{K}^*$. Note that the submatrix $\mathbf{A}$ of $\mathbf{K}_T^{RS}$ is known from the Newton–Raphson iteration and decomposed there. As mentioned in the previous sections by re-arranging we obtain without additional computational costs a decomposition of $\mathbf{A}$.

Box 3. Algorithm 3

(a) Build the tangent stiffness matrix of the reduced system, do not follow any boundary condition.

(b) Add all global boundary conditions of the structure which are also relevant for the divided structure. Denote the resulting tangent stiffness matrix by $\mathbf{K}_T^S$ as in equation (61).

(c) Use a decomposition of $\mathbf{A}$ (known from the Newton–Raphson iteration) to check that $\mathbf{A}$ is positive-definite and compute $\mathbf{S} := \mathbf{D} - \mathbf{C}\mathbf{A}^{-1}\mathbf{B}$.

(d) Compute $\mathbf{K}^* := \sum_{j=1}^{m} \mathbf{T}_j^T \mathbf{S} \mathbf{T}_j$ and decomposition of $\mathbf{K}^*$.

(e) *Output.* If the all pivots in (c) and (d) are positive, then $\mathbf{K}_T$ is positive-definite; the total system is stable. If some pivot in (c) or (d) becomes zero or negative, $\mathbf{K}_T$ is singular or the total system is unstable.

The following corollary gives the relation between the zero-eigenvectors of the full system and the zero-eigenvectors of $\mathbf{K}^*$.

Corollary 1. *If the reduced system is stable but there exists a zero-eigenvectors* $\boldsymbol{\phi}$ *of* $\mathbf{K}^*$ *then*

$$(\boldsymbol{\varphi}_1, \ldots, \boldsymbol{\varphi}_m, \boldsymbol{\phi})^T \tag{65}$$

is a zero-eigenvector of $\mathbf{K}_T$, *where*

$$\boldsymbol{\varphi}_j := -\mathbf{A}^{-1}\mathbf{B}\mathbf{T}_j\boldsymbol{\phi} \quad (j = 1, \ldots, m) \tag{66}$$
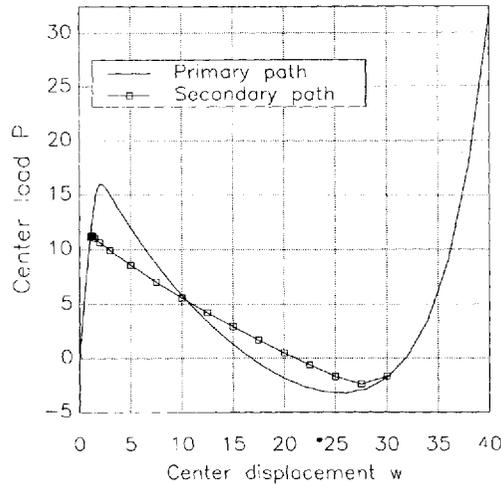
Figure 9. Three-dimensional beam problem: λ–w_3, primary and secondary branch

Proof. With the definition of φ_j there holds

$$\mathbf{K}_T(\varphi_1, \ldots, \varphi_m, \phi)^T = \begin{pmatrix} \mathbf{A}\varphi_j + \mathbf{B}\mathbf{T}_j\phi \\ \sum_{j=1}^{m} \mathbf{T}_j^T \mathbf{C}\varphi_j + \sum_{j=1}^{m} \mathbf{T}^{Tj}\mathbf{D}\mathbf{T}_j\phi \end{pmatrix} = 0 \qquad (67)$$

∎

The following two examples conclude this section and illustrate the theoretical results as well as the improvement of computational efficiency.

Example. Based on the above-introduced analysis in the previous example we can find a symmetry breaking bifurcation point at ($\lambda = 11 \cdot 04$, $w_3 = 1 \cdot 07$) (see Figure 9).

Due to the special material parameters we have a bifurcation point with three zero eigenvalues. The first and second zero-eigenvectors are governed by vertical displacements of the three members, see Figure 10. The third zero-eigenvector of Figure 10 is constructed by a rotation around the vertical axis. The bifurcation points coincides by reason of $EI_y = EI_z$. The symmetric fourth eigenvector which describes the deformation behaviour at the limit point is not a zero-eigenvector.

Remark. The estimation of the computational effort of a combined solution procedure of Algorithm 1 including Algorithm 3 for the part 'stability considerations' is very difficult because it depends highly on the topology of the structure. Therefore, only an approximation of the computational costs can be achieved as follows. Assume that $\dim \mathbf{K}_T = \dim \mathbf{K}_T^{RS}$ such that the decomposition of $\mathbf{K}_T^{RS}$ and $\mathbf{K}_T$ require the costs c and κc, respectively, where (as in Section 1)

$$m \leqslant \kappa \leqslant m^3 \qquad (68)$$

As explained above, the computational costs are reduced by the proposed procedure by a factor

$$\eta = \frac{5c + c'}{5\kappa c} \qquad (69)$$

where c' are the costs for Algorithm 3 which are calculated in the sequel. The additional tasks are in step (c) and (d). Let $k := \dim \mathbf{K}^*$, $r := \dim \mathbf{S} = \dim \mathbf{D}$, $l := \dim \mathbf{A}$. Assume that r, k are very small
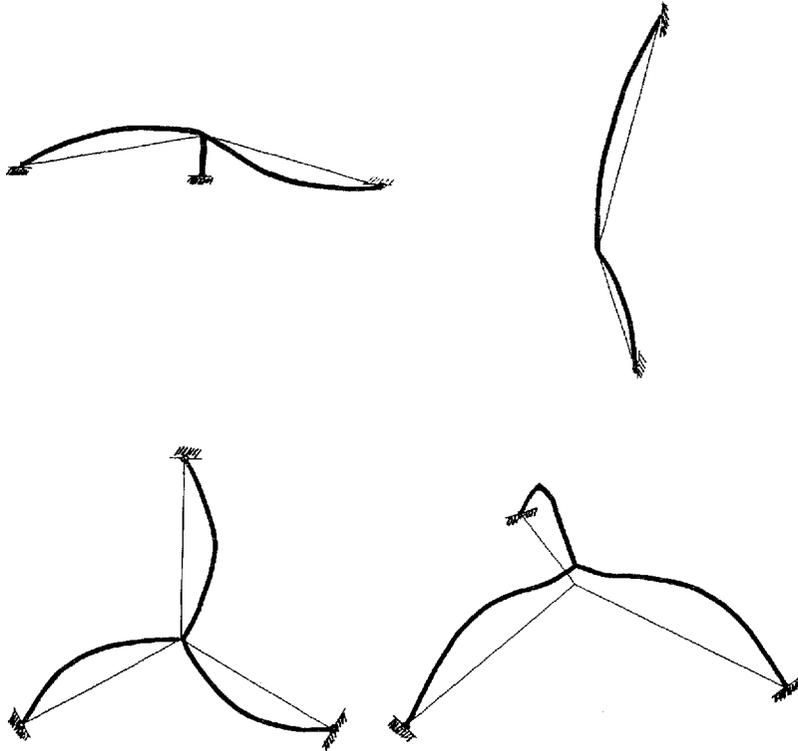
Figure 10. Three-dimensional beam problem: 1–4 eigenvector at the bifurcation point

in comparison with $l \approx n/m$. In the above example we have $l = 33$, $r = k = 6$. As mentioned above, the decomposition of **A** is obtained without further computational costs such that the computation of **S** needs r backward substitutions of vectors with dimension l and $r^2 \cdot l$ operations for the multiplication and r^2 subtractions. Since $r \ll l$ we can neglect the computational costs of step (d) and obtain

$$c' = r^2 \cdot l \leqslant c \tag{70}$$

Note that this is a rough estimate. Therefore, from equation (69) the estimate

$$\eta \leqslant \frac{6}{5m} = 0.4 \tag{71}$$

is concluded for $m = 3$.

Example. Another example to investigate symmetries defined by substructures is a hexagonal star-shaped dome which has been studied in different forms extensively in the literature.[2, 16, 17] Here we consider the problem with the geometrical data from References 2 and 17. In difference to Reference 16 all free nodes are loaded by vertical loads. Figure 11 shows the complete and the reduced system. Due to the description in the mathematical literature, an unrealistic membrane stiffness of $EA = 1$ is chosen.

Here we want to demonstrate the ability to find symmetry-breaking bifurcation points by monitoring the reduced system. For this purpose we show in Figure 12 the first part of the primary load–deflection path with one limit point and three symmetry-breaking bifurcation
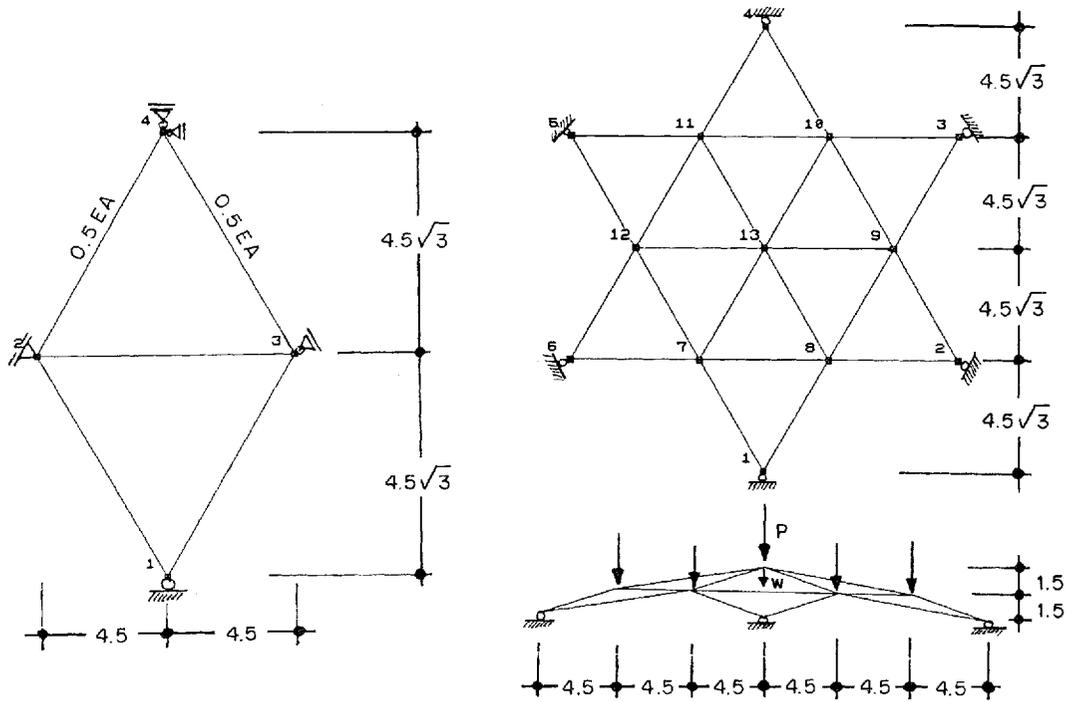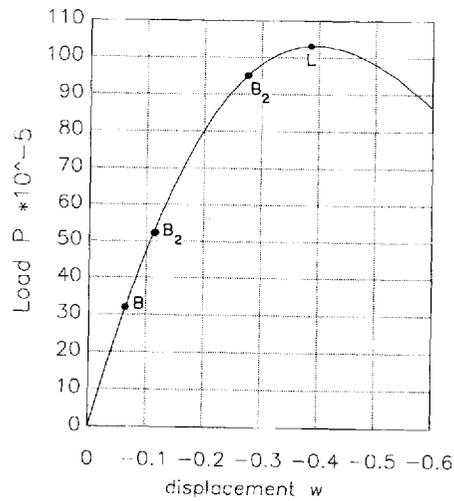
Figure 11. Hexagonal star-shaped dome

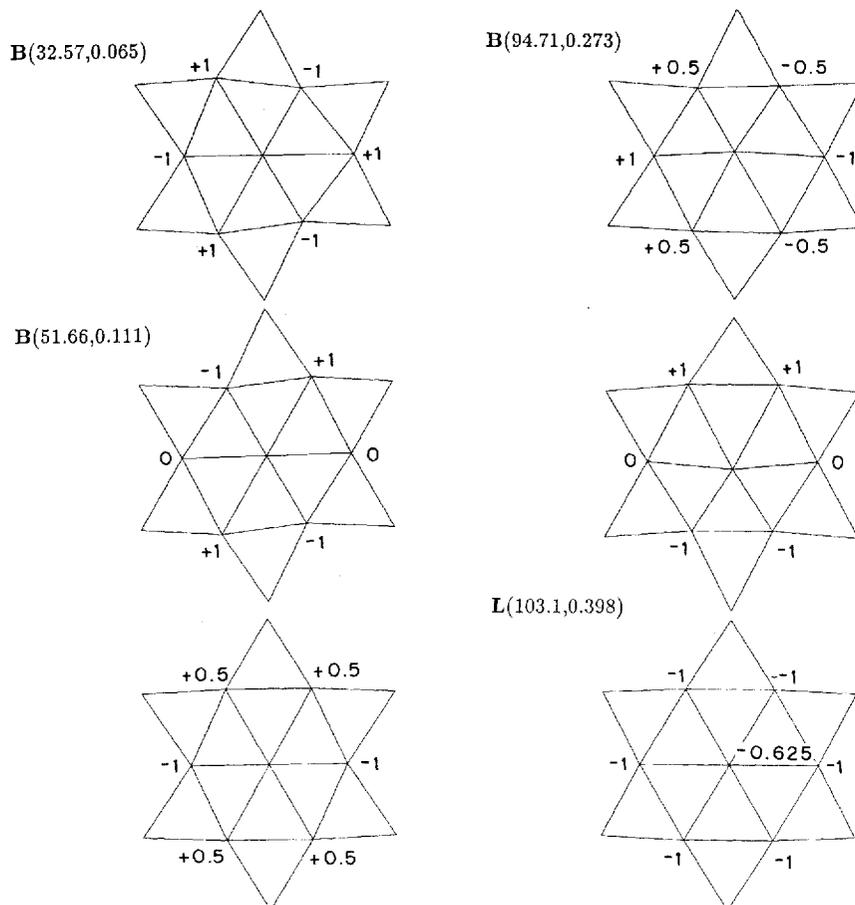Figure 12. First part of the primary path λ–w

Figure 13. Null-eigenvectors at singular points of a hexagonal star

points. The complete load–deflection curve can be found, e.g., in Reference 17. We emphasize that all the stability points shown in Figure 12 as well as the related multiplicities of eigenvalues can be computed only using the very simple reduced system in Figure 11 and the analysis from Algorithm 3.

The special antisymmetric behaviour of the eigenvectors at the bifurcation points and the symmetric eigenvector at the limit point can be seen in Figure 13.

6. CONCLUSIONS

In this paper the effective numerical treatment of symmetry breaking is discussed using the symmetry of the complete system to save computational effort. The engineering notion of a symmetric reduced system is formulated more formally and some relations between the complete symmetric and reduced system are described based on a substructure technique. An efficient algorithm is derived for the important detection of any stability point, in particular, for symmetry-breaking bifurcation points, of the symmetric primary path.

In the presence of reflection symmetries, the additional calculations can easily be implemented in existing computer programs. The case of rotational symmetries is developed in detail and tested in numerical examples.

In all cases the reduction of computational costs is large and nearly equal to the reduction of the degrees of freedom comparing the complete and the reduced system, although some minor additional calculations are required.

REFERENCES

1. T. J. Healey, 'Global symmetry and continuation in the presence of symmetry with an application to solid mechanics', *SIAM J. Math. Anal.* **19**, 824–840 (1988).
2. T. J. Healey, 'A group-theoretic approach to computational bifurcation problems with symmetry', *Comput. Methods Appl. Mech. Eng.*, **67**, 257–295 (1988).
3. W. Wagner and P. Wriggers, 'A simple method for the calculation of postcritical branches', *Eng. Comput.*, **5**, 103–109 (1988).
4. E. Riks, 'The application of Newtons method to the problem of elastic stability', *J. Appl. Mech.*, **39**, 1060–1066 (1972).
5. H. B. Keller, 'Numerical solution of bifurcation and nonlinear eigenvalue problems', in P. Rabinowitz (ed.), *Application of Bifurcation Theory*, Academic Press, New York, 1977, pp. 359–384.
6. E. Ramm, 'Strategies for tracing the nonlinear response near limit points', in W. Wunderlich, E. Stein and K.-J. Bathe (eds.), *Non-linear Finite Element Analysis in Structural Mechanics*, Springer, Berlin, Heidelberg, New York, 1981, pp. 63–89.
7. L. Brezzi, J. Rappaz and P. A. Raviart, 'Finite dimensional approximation of nonlinear problems', *Numer Math.*, **38**, 1–30 (1981).
8. B. Werner and A. Spence, 'The computation of symmetry-breaking bifurcation points', *SIAM J. Numer Anal.*, **21**, 388–399 (1984).
9. M. Golubitsky, I. Stewart and D. G. Schaeffer, *Singularities and Groups in Bifurcation Theory*, Vol. II, Spinger, New York, 1988.
10. O. C. Zienkiewicz and R. L. Taylor, *The Finite Element Method*, 4th edn. Vol. 1 and 2, McGraw-Hill, London, 1989.
11. E. Stein, W. Wagner and P. Wriggers, 'Concepts of modeling and discretization of elastic shells for nonlinear finite element analysis', in J. R. Whiteman (ed.), *Proc. Mathematics of Finite Elements and Applications VI MAFELAP 1987 Conference*, Academic Press, London, 1988, pp. 205–232.
12. W. Wagner, 'Zur Formulierung eines Zylinderschalenelementes mit vollständig reduzierter Integration', *ZAMM* **68**, T430–433 (1988).
13. G. Horrigmoe, 'Finite element analysis of free-form shells', *Report No. 77-2*, Institute for Statikk, Division of Structural Mechanics, The Norwegian Institute of Technology, University of Trondheim, Norway.
14. A. K. Noor, 'Recent advances in reduction methods for nonlinear problems', *Comput. Struct.*, **13**, 31–44 (1981).
15. W. Wagner, 'Zur Behandlung von Stabilitätsproblemen der Elastostatik mit der Methode der Finiten Elemente', *Forschungs- und Seminarberichte aus dem Bereich der Mechanik der Universität Hannover*, F91/1 (1991)
16. P. Wriggers, W. Wagner and C. Miehe, 'A quadratically convergent procedure for the calculation of stability points in finite element analysis', *Comput. Methods Appl. Mech. Eng.*, **70**, 329–347 (1988).
17. P. C. Stork and B. Werner, 'Symmetry adapted block diagonalization in equivariant steady state bifurcation problems and its numerical application', *Adv. Math.* (to appear).